NASA Technical Memorandum 80118

NASA-TM-80118 19790019761

ON THE ATTENUATION OF SOUND BY THREE-DIMENSIONALLY SEGMENTED ACOUSTIC LINERS IN A RECTANGULAR DUCT

W. Koch

June 1979

National Aeronautics and Space Administration

Langley Research Center
Hampton, Virginia 23665

1 Report No	2 Government Accession No	3 Recipient's Catalog No
NASA TM-80118		

4 Title and Subtitle	5 Report Date
On the Attenuation of Sound By Three-Dimensionally Segmented Acoustic Liners in A Rectangular Duct	June 1979
	6 Performing Organization Code
7 Author(s)	8 Performing Organization Report No
W. Koch*	
9 Performing Organization Name and Address	10 Work Unit No
NASA Langley Research Center Hampton, Virginia 23665	505-03-13-18
	11 Contract or Grant No
	13 Type of Report and Period Covered
12 Sponsoring Agency Name and Address	Technical Memorandum
National Aeronautics and Space Administration Washington, D.C. 20546	14 Sponsoring Agency Code

15 Supplementary Notes

*Institut für Theoretische Strömungsmechanik, DFVLR/AVA Göttingen, Bunsenstrasse 10, D-34 Göttingen, Federal Republic of Germany

16 Abstract

Axial segmentation of acoustically absorbing liners in rectangular, circular or annular duct configurations has proven to be a very useful concept to obtain higher noise attenuation with respect to the bandwidth of absorption as well as the maximum attenuation. As a consequence, advanced liner concepts have been proposed which induce a modal energy transfer in both cross-sectional directions to further reduce the noise radiated from turbofan engines. However, these advanced liner concepts require three-dimensional geometries which are difficult to treat theoretically. In the present paper, a very simple three-dimensional problem is investigated analytically. The results show a strong dependence on the positioning of the liner for some incident source modes while the effect of three-dimensional segmentation appears to be negligible over the frequency range considered.

17 Key Words (Suggested by Author(s))

Duct Acoustics
Sound Attenuation
Segmented Acoustic Liners

18 Distribution Statement

Unclassified - Unlimited

Subject Category 71

19 Security Classif (of this report)	20 Security Classif (of this page)	21 No of Pages	22 Price*
Unclassified	Unclassified	27	$4.50

ON THE ATTENUATION OF SOUND BY THREE-DIMENSIONALLY SEGMENTED ACOUSTIC LINERS IN A RECTANGULAR DUCT †

W. Koch
Institut für Theoretische Strömungsmechanik,
DFVLR/AVA Göttingen,
Bunsenstrasse 10, D-34 Göttingen,
Federal Republic of Germany

SUMMARY

Axial segmentation of acoustically absorbing liners in rectangular, circular or annular duct configurations has proven to be a very useful concept to obtain higher noise attenuation with respect to the bandwidth of absorption as well as the maximum attenuation. As a consequence, advanced liner concepts have been proposed which induce a modal energy transfer in both cross-sectional directions to further reduce the noise radiated from turbofan engines. However, these advanced liner concepts require three-dimensional geometries which are difficult to treat theoretically. In the present paper, a very simple three-dimensional problem is investigated analytically. The results show a strong dependence on the positioning of the liner for some incident source modes while the effect of three-dimensional segmentation appears to be negligible over the frequency range considered.

---

† This research was conducted while the author held a National Research Council Senior Research Associateship at the NASA Langley Research Center, Hampton, Virginia.

INTRODUCTION

In order to meet current and future noise regulations of commercial jet transport aircraft, considerable research effort has been expended over the past years in an attempt to attenuate the noise radiated from turbofan engines. With most design possibilities for minimizing the noise generated at the source being exhausted, acoustic lining became one of the more established approaches to further reduce the noise. Advanced duct liner concepts have been developed in order to achieve more absorption with less weight and volume of acoustic treatment starting with the concept of axially segmented liners originally introduced by Lansing and Zorumski [1]. Several theoretical and experimental investigations have proved that multi-segmented liners can be superior to uniform liners with regard to the bandwidth of absorption as well as the maximum attenuation. The basic idea behind the concept is that the impedance discontinuities of the various segments are used to redistribute the acoustic energy into different, usually higher order, acoustic modes which are absorbed more efficiently. Of course, the results are strongly dependent upon the given sound source.

In [1], as well as most other papers treating multisegmented liners (see for example [2], [3], [4]), either two-dimensional or annular duct geometries have been employed which resulted in one mode number remaining constant. From the fact that, in an annular lined duct, the attenuation is higher not only for higher order radial but also for higher order circumferential modes, it is only natural to expect higher attenuation if the modal structure is broken up in <u>both</u> mode numbers since then several more modes are available for an energy transfer. The use of circumferentially as well as axially segmented liners leading ultimately to the concept of liners with continuously varying impedance in all directions is based upon

this idea. Aside from manufacturing difficulties, the main problem with these advanced liner concepts is that they involve three-dimensional geometries which are difficult to treat theoretically.

The present investigation is a first attempt to examine the effects of three-dimensional segmentation analytically. By looking at a very simple three-dimensional problem, namely two axially segmented uniform liner pairs which are tilted by 90 degrees with respect to each other in an otherwise infinitely long, hard walled rectangular duct, the effect of modal break up in both cross-sectional directions can be studied. At the same time, this problem constitutes an excellent testing ground for the analytical approach of combining the mode matching and Wiener-Hopf technique. This method is very useful in solving certain three-dimensional problems by matching essentially two-dimensional solutions. Disappointingly, the few sample results that were evaluated numerically show practically no increase in sound attenuation due to three-dimensional segmentation. Two-dimensional segmentation appears to be equal or even superior in the examples considered as long as the liners are positioned correctly. Thus the results reemphasize the fact that, for a given incident mode, the sound attenuation can be increased substantially if the liner is positioned such that the wave front normal points into the liner.

GOVERNING EQUATIONS

The geometry of the problem is schematically depicted in Figure 1. In an infinitely long, hard walled rectangular duct of constant cross-section, W x H, two liner pairs, separated by a distance $\Delta L = L_2 - L_1$, are mounted on the side walls and are tilted by 90 degrees with respect to each other. A uniform axial mean flow of Mach number $M = W_\infty/a_\infty \geq 0$ is assumed in the positive x - direction. Viscosity, thermal conductivity and all nonlinearities are

ignored. Introducing a dimensionless perturbation velocity potential Φ_o such that

$$\underline{v}_t = U_{ref}\,(\underline{i} + \underline{v}); \qquad \underline{v} = L_{ref}\ \text{grad}\ \Phi_o \quad , \tag{1}$$

the governing convected wave equation is

$$\left\{ \frac{\partial^2}{\partial X^2} + \frac{\partial^2}{\partial Y^2} + \frac{\partial^2}{\partial Z^2} - \frac{1}{a_\infty^2}\ \frac{D^2}{Dt^2} \right\} \Phi_o = 0, \tag{2}$$

where

$$\frac{D}{Dt} = \frac{\partial}{\partial t} + W_\infty\ \frac{\partial}{\partial X} \quad ,$$

with the corresponding expression for the perturbation pressure p

$$p_t = p_\infty\,(1 + p); \qquad p = -\frac{\kappa\, U_{ref}\, L_{ref}}{a_\infty^2}\ \frac{D}{Dt}\ \Phi_o \ .$$

L_{ref} is a reference length (in our case, the duct height H) while the reference velocity U_{ref} is taken to be the uniform mean flow velocity W_∞, if mean flow is present, or the ambient sound speed a_∞ if the undisturbed medium is at rest. The sound source is assumed to have harmonic time dependence $\exp(i\omega t)$.

After applying a Prandtl-Glauert type transformation and simultaneously nondimensionalizing the spatial coordinates

$$x = \frac{X}{L_{ref}\sqrt{1 - M^2}} \quad , \quad y = \frac{Y}{L_{ref}} \quad , \quad z = \frac{Z}{L_{ref}} \quad , \tag{3}$$

it is advantageous to introduce the amplitude function $\phi(x,y,z)$ defined by

$$\Phi_o\,(X, Y, Z, t) = \text{Re}\left\{ \phi(x, y, z)\ e^{i(\omega t + K\,Mx)} \right\} \quad , \tag{4}$$

where

$$K = \frac{\omega\, L_{ref}}{a_\infty \sqrt{1 - M^2}} \ .$$

This reduces the governing equation (2) to the Helmholtz equation

$$\left\{ \frac{\partial^2}{\partial x^2} + \frac{\partial^2}{\partial y^2} + \frac{\partial^2}{\partial z^2} + K^2 \right\} \phi = 0$$

which has to be solved for the axially segmented liner configurations shown in Figure 2 in nondimensionalized notation, i.e. $h = H/L_{ref}$, $w = W/L_{ref}$ and $\ell = L/(L_{ref}\sqrt{1 - M^2})$. In Figure 2a, the two liner pairs are mounted on the same side walls while the remaining two walls are hard. This is a two-dimensional configuration since the mode number in the y-direction does not change throughout the whole lined section. In Figure 2b, the second liner pair is tilted by 90 degrees. It is this three-dimensional configuration we are mainly interested in here.

In the hard walled sections I, II and III (see Figure 2) the sound field can be described by the sum of acoustic modes $\Psi_{m,n}(y,z)$. The method of separation of variables together with the application of the hard wall boundary condition of zero normal velocity leads to (cf. [2])

$x \leq 0$:

$$\phi^{(I)}(x, y, z) = \vec{E}_{r,s}\, e^{i\gamma_{r,s}x}\, \Psi_{r,s}(y, z) + \sum_{m=0}^{\infty} \sum_{n=0}^{\infty} \overleftarrow{A}^{(1)}_{m,n}\, e^{-i\gamma_{m,n}x}\, \Psi_{m,n}(y, z),$$

$\ell_1 \leq x \leq \ell_2$:

$$\phi^{(II)}(x, y, z) = \sum_{m=0}^{\infty} \sum_{n=0}^{\infty} \vec{B}^{(1)}_{m,n}\, e^{i\gamma_{m,n}(x - \ell_1)}\, \Psi_{m,n}(y, z) + \sum_{m=0}^{\infty} \sum_{n=0}^{\infty} \overleftarrow{A}^{(2)}_{m,n}\, e^{-i\gamma_{m,n}(\ell_2 - x)}\, \Psi_{m,n}(y, z),$$

$x \geq \ell_2$:

$$\phi^{(III)}(x, y, z) = \sum_{m=0}^{\infty} \sum_{n=0}^{\infty} \vec{B}^{(2)}_{m,n}\, e^{i\gamma_{m,n}(x - \ell_3)}\, \Psi_{m,n}(y, z) + \overleftarrow{E}_{r,s}\, e^{-i\gamma_{r,s}(x - \ell_3)}.$$

Here the hard wall duct eigenfunctions and eigenvalues are

$$\Psi_{m,n}(y, z) = \cos(K_m y) \cos(K_n z) \quad ,$$

where

$$K_m = \frac{m \Pi L_{ref}}{W} = \frac{m \Pi}{w} \; ; \quad K_n = \frac{n \Pi L_{ref}}{H} = \frac{n \Pi}{h} \text{ and } K_{m,n}^2 = K_m^2 + K_n^2 \quad .$$

Assuming only a single incident duct wave (due to the linearity, the solutions can always be superimposed), $\vec{E}_{r,s}$, $\overleftarrow{E}_{r,s}$ denote the modal amplitudes of the prescribed incoming hard wall duct waves impinging from upstream and downstream respectively. $\vec{A}_{m,n}(\nu)$, $\overleftarrow{A}_{m,n}(\nu)$, and $\vec{B}_{m,n}(\nu)$, $\overleftarrow{B}_{m,n}(\nu)$ are the modal amplitudes of the waves in front of and behind the ν-th lined segment, propagating upstream or downstream (see Figure 2).

$$\gamma_{m,n} = \begin{cases} -\hat{\gamma}_{m,n} \equiv -\sqrt{K^2 - K_{m,n}^2} \; , & K > K_{m,n} \\ \tilde{\gamma}_{m,n} \equiv i\sqrt{K_{m,n}^2 - K^2} \; , & K < K_{m,n} \end{cases}$$

are the corresponding modal propagation constants. For $K < K_{m,n}$, the duct wave is attenuated (cut off) while for $K > K_{m,n}$ the duct wave propagates. In the latter case one has to distinguish two cases (cf. [2]):

a) $K > K_{m,n} / \sqrt{1 - M^2}$: The corresponding phase velocities have different signs for the upstream and downstream propagating wave.

b) $K_{m,n} < K < K_{m,n} / \sqrt{1 - M^2}$: The two phase velocities have the same sign and energy considerations are necessary to determine the direction of wave propagation (see [5] or [6], p. 161).

For the lined sections, a locally reacting lining material of specific normal acoustic impedance ζ_w is assumed. For our numerical examples, the crossover frequency impedance model

$$\zeta_w = R_* \, (1 + i \, f_*/f_{0*}) - i \, \mathrm{ctg} \, (2\pi \, f_* \, d_*) \qquad (5)$$

for honeycomb liners with an impervious backing and a thin sheet of absorptive facing material is employed. R_* and $f_{0*} = f_0 L_{ref}/a_\infty$ are the specific acoustic resistance and the nondimensional characteristic frequency (crossover frequency) of the facing sheet while $d_* = d/L_{ref}$ is the dimensionless depth of the honeycomb structure. $f_* = f \, L_{ref}/a_\infty$ denotes the frequency parameter.

Since we allow a uniform mean flow, the medium inside and outside the liner is assumed to be separated by an infinitely thin vortex sheet of finite axial length across which the pressure remains continuous. Furthermore, the kinematic condition of equal particle displacement on both sides of the vortex sheet must be imposed. The solution of the problem of sound transmission through a finite length acoustically treated duct section is assumed to be known in terms of the various reflection and transmission factors $R_{m,n;\mu,\nu}$ and $T_{m,n;\mu,\nu}$. The details of the solution are unimportant as far as the present work is concerned to the extent that the finite length liner can be taken as a "black box" with known reflection and transmission characteristics.

GENERAL FORMULATION IN TERMS OF THE MODAL REFLECTION AND TRANSMISSION FACTORS

The concept of reflection and transmission factors has proven very useful in several engineering disciplines. In acoustics, most muffler design procedures are based on the one-dimensional transmission-line approximation and a very nice introduction to multidimensional problems in ducts was given by Zorumski [7]. The reflection and transmission factors relate the modal amplitudes in front of and behind a nonuniform duct section. This nonuniform duct section may be a discontinuity in the physical properties, like a change in duct cross section or wall admittance, or may be of finite axial extent. In this paper, we are mainly concerned with the latter. Referring to a simple liner pair in Figure 2,

$\vec{R}_{m,n;\mu,\nu}$, for example, denotes the complex amplitude of the (m,n) th reflected wave due to a unit amplitude (μ,ν) th wave impinging from upstream. Similarly $\vec{T}_{m,n;\mu,\nu}$ denotes the complex amplitude of the (m,n) th transmitted wave due to a unit amplitude (μ,ν) th wave impinging from upstream. Similar definitions apply for the incident wave coming from downstream indicated by a left pointing arrow in the superscript.

If all four walls of the two lined sections in Figure 2 are treated with acoustic material, one can write for the first lined section

$$\overleftarrow{A}^{(1)}_{m,n} = \vec{E}_{r,s}\,\vec{R}^{(1)}_{m,n;r,s} + \sum_{\mu=0}^{\infty}\sum_{\nu=0}^{\infty}\overleftarrow{B}^{(1)}_{\mu,\nu}\,\overleftarrow{T}^{(1)}_{m,n;\mu,\nu}\ , \tag{6a}$$

$$\vec{B}^{(1)}_{m,n} = \vec{E}_{r,s}\,\vec{T}^{(1)}_{m,n;r,s} + \sum_{\mu=0}^{\infty}\sum_{\nu=0}^{\infty}\overleftarrow{B}^{(1)}_{\mu,\nu}\,\overleftarrow{R}^{(1)}_{m,n;\mu,\nu}\ , \tag{6b}$$

and similarly for the second liner segment

$$\overleftarrow{A}^{(2)}_{m,n} = \sum_{\mu=0}^{\infty}\sum_{\nu=0}^{\infty}\vec{A}^{(2)}_{\mu,\nu}\,\vec{R}^{(2)}_{m,n;\mu,\nu} + \overleftarrow{E}_{r,s}\,\overleftarrow{T}^{(2)}_{m,n;r,s} \tag{7a}$$

$$\vec{B}^{(2)}_{m,n} = \sum_{\mu=0}^{\infty}\sum_{\nu=0}^{\infty}\vec{A}^{(2)}_{\mu,\nu}\,\vec{T}^{(2)}_{m,n;\mu,\nu} + \overleftarrow{E}_{r,s}\,\overleftarrow{R}^{(2)}_{m,n;r,s}\ . \tag{7b}$$

With zero mean flow the reflection (and transmission) factors $\vec{R}^{(\nu)}_{m,n;\mu,\nu}$ and $\overleftarrow{R}^{(\nu)}_{m,n;\mu,\nu}$ are equal. Throughout the intermediate hard walled section II, each mode propagates independently such that

$$\vec{A}^{(2)}_{m,n} = \vec{B}^{(1)}_{m,n}\ e^{i\gamma_{m,n}(\ell_2-\ell_1)}\ , \tag{8a}$$

$$\overleftarrow{B}^{(1)}_{m,n} = \overleftarrow{A}^{(2)}_{m,n}\ e^{-i\gamma_{m,n}(\ell_2-\ell_1)}\ . \tag{8b}$$

Equations (8) can be used to eliminate $\vec{A}^{(2)}_{m,n}$ and $\overleftarrow{B}^{(1)}_{m,n}$ in (6) and (7). Then (6b) and (7a) constitute a two-fold infinite set of determination equations for the two-fold set of infinitely many unknown amplitudes $\vec{B}^{(1)}_{m,n}$ and $\overleftarrow{A}^{(2)}_{m,n}$;

$m,n = 0, 1, 2, \ldots,$

$$\vec{B}^{(1)}_{m,n} - \sum_{\mu=0}^{\infty} \sum_{\nu=0}^{\infty} \overleftarrow{A}^{(2)}_{\mu,\nu} e^{-i\gamma_{\mu,\nu}(\ell_2 - \ell_1)} \overleftarrow{R}^{(1)}_{m,n;\mu,\nu} = \vec{E}_{r,s} \vec{T}^{(1)}_{m,n;r,s} \tag{9a}$$

and

$$- \sum_{\mu=0}^{\infty} \sum_{\nu=0}^{\infty} \vec{B}^{(1)}_{\mu,\nu} e^{i\gamma_{\mu,\nu}(\ell_2 - \ell_1)} \vec{R}^{(2)}_{m,n;\mu,\nu} + \overleftarrow{A}^{(2)}_{m,n} = \overleftarrow{E}_{r,s} \overleftarrow{T}^{(2)}_{m,n;r,s} . \tag{9b}$$

This infinite set of equations can be truncated a few modes beyond the modal cut off numbers. Therefore, once the reflection and transmission factors are known and the source characteristics are prescribed in terms of the incoming modal amplitudes $\vec{E}_{r,s}$ and $\overleftarrow{E}_{r,s}$, the solution of the truncated set of equations (9) is straight forward.

The computation of the reflection and transmission factors constitutes the main problem. Unfortuately, to my knowledge there exist no analytical results for the reflection and transmission factors of three-dimensional rectangular ducts lined uniformly over a finite axial length on all four walls although the mode matching method should provide one means to do so. With regard to numerical techniques, for example, Watson's method [8] could be employed. However, in several applications only two opposing side walls are lined such that one mode number can be held fixed while computing the corresponding reflection and transmission factors. This is the case for the examples depicted in Figure 2. Thus the solution procedure will now be outlined for the special case of two tilted liner pairs.

TWO LINER PAIRS TILTED BY 90 DEGREES WITH RESPECT TO EACH OTHER

In the first lined section of Figure 2b, the walls are hard at $y = 0$ and $y = w$. Hence, for a given incoming mode $\vec{E}_{r,s}$ or $\overleftarrow{B}^{(1)}_{m,n}$, the mode number r or

m in the y-direction will be unaffected by the presence of the first liner and will equal that of the incoming mode. For the quasi-two-dimensional problem shown in Figure 2a, this is true all the way through both lined sections such that r is fixed by the incoming mode. For the second lined section of Figure 2b, the walls at z = 0 and z = h are hard and for a given incoming mode, $\vec{A}^{(2)}_{m,n}$ or $\overleftarrow{E}_{r,s}$, the mode number s or n in z-direction will equal that of the incoming mode. The three-dimensional effect is therefore due to the interaction of the two liner pairs. In the intermediate hard walled section II, an incoming mode $\vec{A}^{(2)}_{\mu,n}$ produces reflected amplitudes $\overleftarrow{A}^{(2)}_{m,n}$ with n = const., while an incoming mode $\overleftarrow{B}^{(1)}_{m,\nu}$ produces reflected amplitudes $\vec{B}^{(1)}_{m,n}$ with m = const. All reflection and transmission factors of the first lined section can be computed by keeping the mode number m constant and equal to that of the corresponding incident mode; and all reflection and transmission factors of the second liner section can be computed by keeping the mode number n constant and equal to that of the relevant incident wave.

Equation (6) can therefore be rewritten in the form

$$\overleftarrow{A}^{(1)}_{m,n} = \delta_{m,r}\,\vec{E}_{r,s}\,\vec{R}^{(1)}_{m,n;r,s} + \sum_{\nu=0}^{\infty} \overleftarrow{B}^{(1)}_{m,\nu}\,\overleftarrow{T}^{(1)}_{m,n;m,\nu} \quad , \tag{10a}$$

$$\vec{B}^{(1)}_{m,n} = \delta_{m,r}\,\vec{E}_{r,s}\,\vec{T}^{(1)}_{m,n;r,s} + \sum_{\nu=0}^{\infty} \overleftarrow{B}^{(1)}_{m,\nu}\,\overleftarrow{R}^{(1)}_{m,n;m,\nu} \quad . \tag{10b}$$

Here $\delta_{m,n}$ denotes Kronecker's delta function.

Similarly equations (7) become

$$\overleftarrow{A}^{(2)}_{m,n} = \sum_{\mu=0}^{\infty} \vec{A}^{(2)}_{\mu,n}\,\vec{R}^{(2)}_{m,n;\mu,n} + \delta_{n,s}\,\overleftarrow{E}_{r,s}\,\overleftarrow{T}^{(2)}_{m,n;r,s} \quad , \tag{11a}$$

$$\vec{B}^{(2)}_{m,n} = \sum_{\mu=0}^{\infty} \vec{A}^{(2)}_{\mu,n}\,\vec{T}^{(2)}_{m,n;\mu,n} + \delta_{n,s}\,\overleftarrow{E}_{r,s}\,\overleftarrow{R}^{(2)}_{m,n;r,s} \quad . \tag{11b}$$

Again employing the uniform duct transmission equations (8), the infinite system (9) now reduces to the special form

$$\vec{B}^{(1)}_{m,n} - \sum_{\nu=0}^{\infty} \overleftarrow{A}^{(2)}_{m,\nu} \; e^{-i\gamma_{m,\nu}(\ell_2 - \ell_1)} \; \overleftarrow{R}^{(1)}_{m,n;m,\nu} = \delta_{m,r} \vec{E}_{r,s} \vec{T}^{(1)}_{m,n;r,s} \quad ,$$

$$- \sum_{\mu=0}^{\infty} \vec{B}^{(1)}_{\mu,n} \; e^{i\gamma_{\mu,n}(\ell_2 - \ell_1)} \; \vec{R}^{(2)}_{m,n;\mu,n} + \overleftarrow{A}^{(2)}_{m,n} = \delta_{n,s} \overleftarrow{E}_{r,s} \overleftarrow{T}^{(2)}_{m,n;r,s} \quad ,$$

$$m,n = 0, 1, 2, \ldots \; .$$

r,s are the prescribed mode numbers of the incident waves. Using matrix partitioning this set of equations may be written

$$\left[\begin{array}{c|c} [\,\delta_{m+n,\,\mu+\nu}\,] & -[\,\delta_{m,\mu} e^{-i\gamma_{\mu,\nu}(\ell_2 - \ell_1)} \overleftarrow{R}^{(1)}_{m,n;\mu,\nu}] \\ \hline -[\,\delta_{n,\nu} e^{i\gamma_{\mu,\nu}(\ell_2 - \ell_1)} \vec{R}^{(2)}_{m,n;\mu,\nu}\,] & [\,\delta_{m+n,\,\mu+\nu}\,] \end{array}\right] \left\{\begin{array}{c} \vec{B}^{(1)}_{\mu,\nu} \\ \hline \overleftarrow{A}^{(2)}_{\mu,\nu} \end{array}\right\} =$$

$$\left\{\begin{array}{c} \{\delta_{m,r} \vec{T}^{(1)}_{m,n;r,s} \vec{E}_{r,s}\} \\ \hline \{\delta_{n,s} \overleftarrow{T}^{(2)}_{m,n;r,s} \overleftarrow{E}_{r,s}\} \end{array}\right\} \quad . \qquad (12)$$

NUMERICAL RESULTS

The quantities of most practical interest are the reflection and transmission coefficients. These are the ratio of the reflected or transmitted power in the (m,n)th cut on mode over the incident power in the (r,s)th cut on mode. For an (r,s) duct wave incident from upstream, they are defined by

$$\vec{\rho}_{m,n;r,s} = \frac{K_{m,n}\,(2-\delta_{o,r})\,(2-\delta_{o,s})}{K_{r,s}\,(2-\delta_{o,m})\,(2-\delta_{o,n})} \left| \frac{\overleftarrow{A}^{(1)}_{m,n}}{\vec{E}_{r,s}} \right|^2 ,$$

$$\vec{\tau}_{m,n;r,s} = \frac{K_{m,n}\,(2-\delta_{o,r})\,(2-\delta_{o,s})}{K_{r,s}\,(2-\delta_{o,m})\,(2-\delta_{o,n})} \left| \frac{\vec{B}^{(2)}_{m,n}}{\vec{E}_{r,s}} \right|^2 .$$

Similar definitions apply for a mode incident from downstream. The total reflected or transmitted power for a single incoming mode (r,s) is then obtained by simply summing the contributions of all cut on (m,n) modes, i.e.

$$\vec{\rho}_{r,s} = \sum_{m,n/\text{cut on}} \vec{\rho}_{m,n;r,s} \quad ; \qquad \vec{\tau}_{r,s} = \sum_{m,n/\text{cut on}} \vec{\tau}_{m,n;r,s} .$$

The acoustic effectivity of a liner combination is usually measured by the power attenuation or insertion loss ΔP. For a single incoming mode (r,s), it is defined by

$$\Delta P\ [\text{dB}] = 10 \log (1/\tau_{r,s}) .$$

In our numerical examples, the mean flow Mach number is taken to be zero such that the relevant reflection and transmission factors for a simple liner pair can be computed by the method outlined in [4]. Originally it was intended to compute the reflection and transmission factors for uniform mean flow ("plug" flow) by extending the Wiener-Hopf method described in [4]. It turned out that the extension is not trivial leading to the appearance of instability waves hitherto neglected in all mode matching approaches. Therefore a more thorough study of the mean flow problem is necessary which will be reported separately.

The infinite set of equations (12) is evaluated numerically by truncating it, in general, three modes beyond the corresponding cut off mode. Valuable computational checks are provided by the requirements that the total transmitted, reflected and absorbed powers have to equal the incident power, i.e.

$$\rho_{r,s} + \tau_{r,s} + \alpha_{r,s} = 1 \quad ,$$

as well as by the reciprocity theorem in the form

$$(2 - \delta_{r,o})\,(2 - \delta_{s,o})\,K_{m,n}\,\frac{\overleftarrow{A}^{(1)}_{m,n}}{\vec{E}_{r,s}} = (2 - \delta_{m,o})\,(2 - \delta_{n,o})\,K_{r,s}\,\frac{\overleftarrow{A}^{(1)}_{r,s}}{\vec{E}_{m,n}} \quad .$$

This reciprocity theorem is valid only for $M = 0$ but applies to cut off modes as well as to cut on modes. The relevant absorption coefficient $\alpha_{r,s}$ can be computed from the solution in the lined section (see [4]).

The numerical examples are chosen such as to provide a comparison with previous results [4] whenever possible. In particular, the two liners in each pair are assumed to be identical and to have the same axial length $L_1/H = \frac{2.17}{2}$. To avoid geometric effects, the duct is assumed to be of square cross section H x H, H = 18.73 cm. The crossover frequency impedance model (5) with $f_{o*} = 8.14$ is used for all examples.

In Figures 3 to 5 the power attenuation is plotted as a function of frequency. First, to check the procedure, the two-dimensional configuration of Figure 2a is evaluated. Assuming an incident fundamental mode (0,0), the result is shown as curve A in Figure 3 and is identical to the one given in [4]. From a computational point of view, the present approach, using mode matching in conjunction with the 3-part Wiener-Hopf technique, is preferential to the n-part Wiener-Hopf approach of [4] because one and the same Wiener-Hopf subroutine can be used for an arbitrary number of lined sections and only the fairly straight forward matrix equation (12) has to be reformulated if more liner sections are added. Also shown in Figure 3

are the results for the case when the two liner pairs are separated by a hard walled section of length L_1 (curve B). Only minor differences are observed due to the interference of waves in the intermediate section. Finally, the second liner pair is tilted by 90 degrees (curve C) and again only minor changes occur. As a matter of fact the power attenuation is even slightly below the one for two-dimensional segmentation over most of the frequency range shown.

In Figure 4, the incident modes (1,0) and (0,1) are considered. Curves A and B show the results for two-dimensional segmentation. Depending on whether the normal wave front vector points into the lined wall (curve B) or is merely tangent (curve A), substantial differences are observed in the power attenuation with a corresponding shift in the tuning frequencies of the two liner segments. Curves C and D show the solution for three-dimensional segmentation, i.e. the second liner pair is tilted. It appears that the effect of correct positioning of the liners by far outweighs the effect of three-dimensional segmentation. Up to the second resonance of the second liner segment at $f_* \approx 2$, the curves for the tilted configuration essentically follow the ones for the corresponding single two-dimensional liner section and then remain at the higher level. Translated to the situation of an annular turbomachinery duct, where mainly circumferential modes are excited, this means that radial liners would be vastly more efficient acoustically than annular liners of the same absorbing area. In a different context, the advantages of the concept of radial liners were pointed out by Abdelhamid [9].

Finally, in Figure 5, the incoming mode is taken to be (1,1) and hence a different liner combination with tuning frequencies above $f_* = 0.7$ had to be chosen. A summary of the cut on frequencies of the various modes for all cases is presented in Table 1. For comparison, the sound attenuation of the

fundamental mode is also included (curve A). Curves B and D give the results for two- and three-dimensional segmentation respectively, for the case with the better impedance match, i.e. the thinner liner is closer to the source. Curves C and E depict the results for the corresponding cases with the two liner segments interchanged. It is somewhat surprising that, even here, the two-dimensionally segmented duct outperforms the duct with three-dimensional segmentation over most of the frequency range, similar to the situation in Figure 3.

CONCLUDING REMARKS

The simple three-dimensional problem of two axially segmented liner pairs tilted by 90 degrees with respect to each other in a rectangular duct was used to study the effect of three-dimensional acoustic liner segmentation. Only a few sample results have been evaluated. However, none of these indicate that the effect of modal energy transfer in both cross-sectional directions can be used to obtain a substantially higher sound attenuation per given liner length. The effect of correct liner positioning, i.e. such that the wave normal points into the liner and is not merely tangential, appears to outweigh the effect of three-dimensional segmentation by far. For the situation of a turbofan exhaust duct, where the sound generation by blade rows leads to the excitation of mainly circumferential modes, this would mean that radial liners are acoustically superior to annular liners.

Although the results with regard to three-dimensional segmentation are very disappointing, the analytical method employed has more far reaching applications already envisaged by Zorumski [7]. In the present paper, the mode matching method is used only to link different finite length sections via the respective transmission and reflection factors. Very often the geometry of those finite length sections is such that only an interaction with one

mode number can occur. In such a case, the various reflection and transmission factors can be computed by two-dimensional methods like the Wiener-Hopf technique. Linking these by means of the mode matching method makes it possible to build up three-dimensional problems by means of two-dimensional solutions. One such example is the interaction of sound generated in a blade row and sound reflected and absorbed by an adjacent liner. Other applications include the interaction of different blade rows (or stages), not only with respect to their acoustics like rotor shielding in turbofan engines or sound transmission through several compressor stages, but also with respect to their aeroelastic behavior since blade vibrations are also communicated via acoustic modes.

ACKNOWLEDGEMENTS

The author is grateful to the National Research Council for the financial support of this investigation and to D. L. Lansing of the Aeroacoustics Branch at the NASA Langley Research Center for providing a stimulating working environment. The editing remarks and several helpful discussions with J. C. Hardin which led to the present approach, and with Y. C. Cho with regard to the reciprocity principle are gratefully acknowledged. Special thanks are due to W. R. Watson for providing his eigenvalue subroutine and to J. P. Mason for computational support

REFERENCES

1. D. L. Lansing and W. E. Zorumski, 1973, Journal of Sound and Vibration 27, 85-100. Effects of wall admittance changes on duct transmission and radiation of sound.

2. D. T. Sawdy, R. J. Beckemeyer and J. D. Patterson, 1976, National Aeronautics and Space Administration Contractor Report CR-134960 (Boeing Document D3-9812-1). Analytical and experimental studies of an optimum multisegment phased liner noise suppression concept.

3. R. E. Motsinger, R. E. Kraft and J. W. Zwick, 1976, American Society of Mechanical Engineers Paper, 76-GT-113. Design of optimum acoustic treatment for rectangular ducts with flow.

4. W. Koch, 1977, Journal of Sound and Vibration, 52, 459-496. Attenuation of sound in multi-element acoustically lined rectangular ducts in the absence of mean flow.

5. W. Eversman, 1971, Journal of the Acoustical Society of America, 50, 421-435. Signal velocity in a duct with flow.

6. B. J. Tester, 1973, Journal of Sound and Vibration, 28, 151-203. The propagation and attenuation of sound in lined ducts containing uniform or "plug" flow.

7. W. E. Zorumski, 1974, National Aeronautics and Space Administration Technical Report TR R-419. Acoustic theory of axisymmetric multisectioned ducts.

8. W. R. Watson, 1977, National Aeronautics and Space Administration Technical Memorandum TM X-74080. A finite element simulation of sound attenuation in a finite duct with a peripherally variable liner.

9. A. N. Abdelhamid, 1977, American Institute of Aeronautics and Astronautics Preprint 77-1357. Augmenting circular silencer performance using lined radial baffles. Presented at the 4th AIAA Aeroacoustics Conference in Atlanta, Georgia, October 3-5, 1977.

LIST OF SYMBOLS

Latin symbols

$A_{m,n}^{(\nu)}$	modal amplitude upstream of ν-th liner segment
a_∞	ambient speed of sound
$B_{m,n}^{(\nu)}$	modal amplitude downstream of ν-th liner segment
$d_* = d/L_{ref}$	dimensionless honeycomb depth
$E_{r,s}$	modal amplitude of incident wave
f	frequency
$f_*=fL_{ref}/a_\infty$	frequency parameter
$f_{o*}=f_oL_{ref}/a_\infty$	reduced characteristic frequency of liner facing sheet
H	duct height
$h = H/L_{ref}$	dimensionless duct height
$i = \sqrt{-1}$	imaginary unit
$\underline{i}$	unit vector in x-direction
$K = \omega L_{ref}/(a_\infty \sqrt{1 - M^2})$	reduced circular frequency parameter
$K_m = m \pi/w$	m-th hard wall eigenvalue in y-direction, m = 0,1,2,...
$K_n = n \pi/h$	n-th hard wall eigenvalue in z-direction, n = 0,1,2,...
$K_{m,n} = \sqrt{K_m^2 + K_n^2}$	
L_1, L_2, L_3	axial lengths; see Figure 1
L_{ref}	reference length ($\equiv H$)
$\ell_1 = L_1/(L_{ref} \sqrt{1 - M^2})$	reduced axial length L_1; see Figure 2
$M = W_\infty/a_\infty$	mean flow Mach number
p	dimensionless acoustic pressure
p_∞	ambient pressure
R_*	specific acoustic resistance of liner facing sheet
$R_{m,n;\mu,\nu}$	(m,n)th modal reflection factor due to (μ,ν)th incident mode

$Re(z)$	real part of z
$T_{m,n;\mu,\nu}$	(m,n)th modal transmission factor due to (μ,ν)th incident mode
t	time
U_{ref}	reference velocity; $U_{ref} = a_\infty$ if $M = 0$, $U_{ref} = W_\infty$ if $M \neq 0$
$\underline{v}$	dimensionless acoustic velocity vector; see equation (1)
W	duct width
W_∞	uniform mean flow velocity
$w = W/L_{ref}$	dimensionless duct width
X, Y, Z	rectangular coordinates
x, y, z	reduced spatial coordinates; see equation (3)

Greek symbols

$$\gamma_{m,n} = \begin{cases} -\hat{\gamma}_{m,n} \equiv -\sqrt{K^2 - K_{m,n}^2}, & K > K_{m,n} \\ \tilde{\gamma}_{m,n} \equiv i\sqrt{K_{m,n}^2 - K^2}, & K < K_{m,n} \end{cases}$$

(m,n)th eigenvalue of hard walled rectangular duct

$\Delta P = 10 \log (1/\tau_{r,s})$	power transmission loss for (r,s)th mode incident
$\delta_{m,n}$	Kronecker's delta; has a value of one if $m = n$ and of zero if $m \neq n$
ζ_w	specific acoustic normal wall impedance; see equation (5)
$\kappa = c_p/c_v$	specific heat ratio
$\rho_{r,s}$	total reflection coefficient for (r,s)th incident mode
$\rho_{m,n;\mu,\nu}$	modal reflection coefficent for (μ,ν)th incident mode
$\tau_{r,s}$	total transmission coefficient for (r,s)th incident mode
$\tau_{m,n;\mu,\nu}$	modal transmission coefficient for (μ,ν)th incident mode

$\Phi_o(X, Y, Z, t)$	dimensional velocity potential; see equation
$\phi(x, y, z)$	amplitude function; see equation (4)
$\Psi_{m,n}(y, z) = \cos(K_m y) \cos(K_n z)$	(m,n)th eigenfunction of hard walled rectangular duct
$\omega = 2\pi f$	circular frequency

Superscripts

$(\overrightarrow{\ })$	quantity referring to wave propagating in the downstream direction
$(\overleftarrow{\ })$	quantity referring to wave propagating in the upstream direction

LEGENDS FOR ILLUSTRATIONS

Figure 1.- Schematic view of two axially segmented duct liner pairs tilted by 90 degrees with respect to each other.

Figure 2.- Geometry of axially segmented liner in nondimensional notion: (a) two-dimensional segmentation; (b) three-dimensional segmentation

Figure 3.- Power attenuation versus frequency with (0,0) mode incident.

Figure 4.- Power attenuation versus frequency with (1,0) or (0,1) mode incident. (Liner data as in Figure 3).

Figure 5.- Power attenuation versus frequency with (0,0) mode, (Curve A), or (1,1) mode incident.

Legend for Table

Table 1.- Cut on frequencies f_* for various modes (m,n) in a square duct (zero mean flow).

m \ n	0	1	2	3	4	5
0	0	0.5	1.0	1.5	2.0	2.5
1	0.5	0.7071	1.1180	1.5811	2.0616	2.5495
2	1.0	1.1180	1.414	1.8028	2.2361	2.6926
3	1.5	1.5811	1.8028	2.1213	2.5	2.9155
4	2.0	2.0616	2.2361	2.5	2.8284	3.2016
5	2.5	2.5495	2.6926	2.9155	3.2016	3.5355

Table 1.- Cut on frequencies f_* for various modes (m,n) in a square duct (zero mean flow).

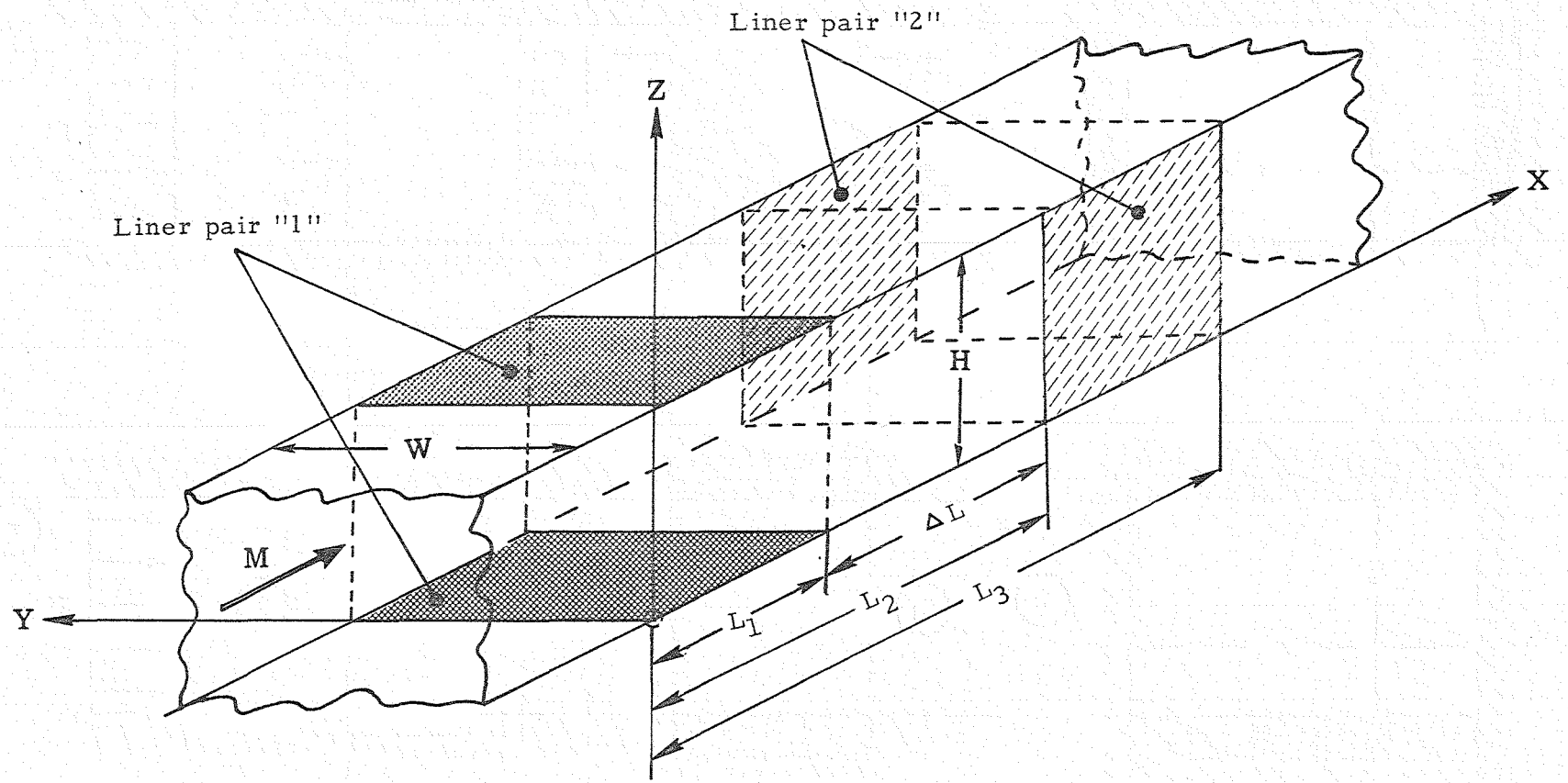

Figure 1.- Schematic view of two axially segmented duct liner pairs tilted by 90 degrees with respect to each other.

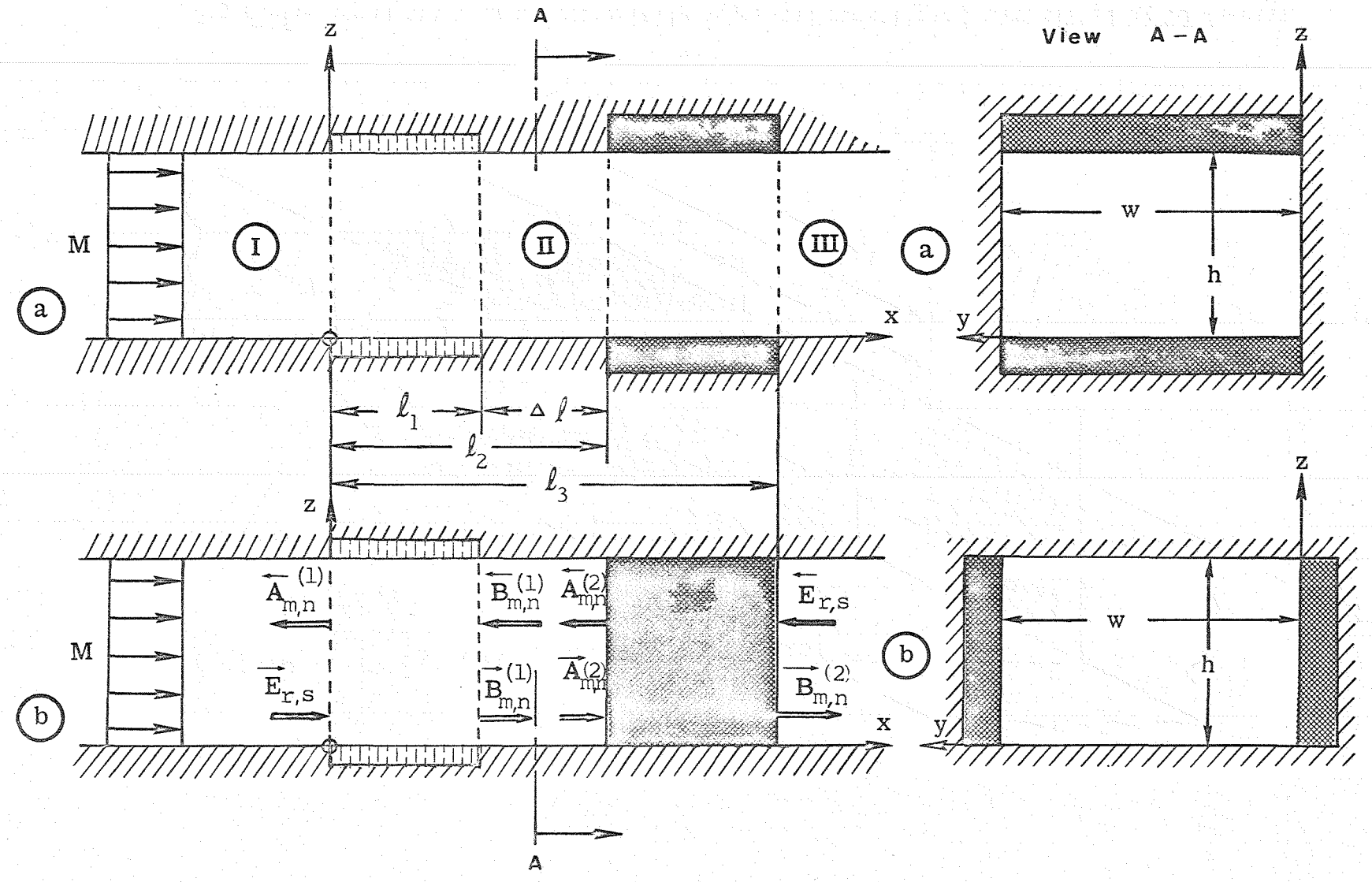

Figure 2.- Geometry of axially segmented liner in nondimensional notation:
(a) two-dimensional segmentation; (b) three-dimensional segmentation

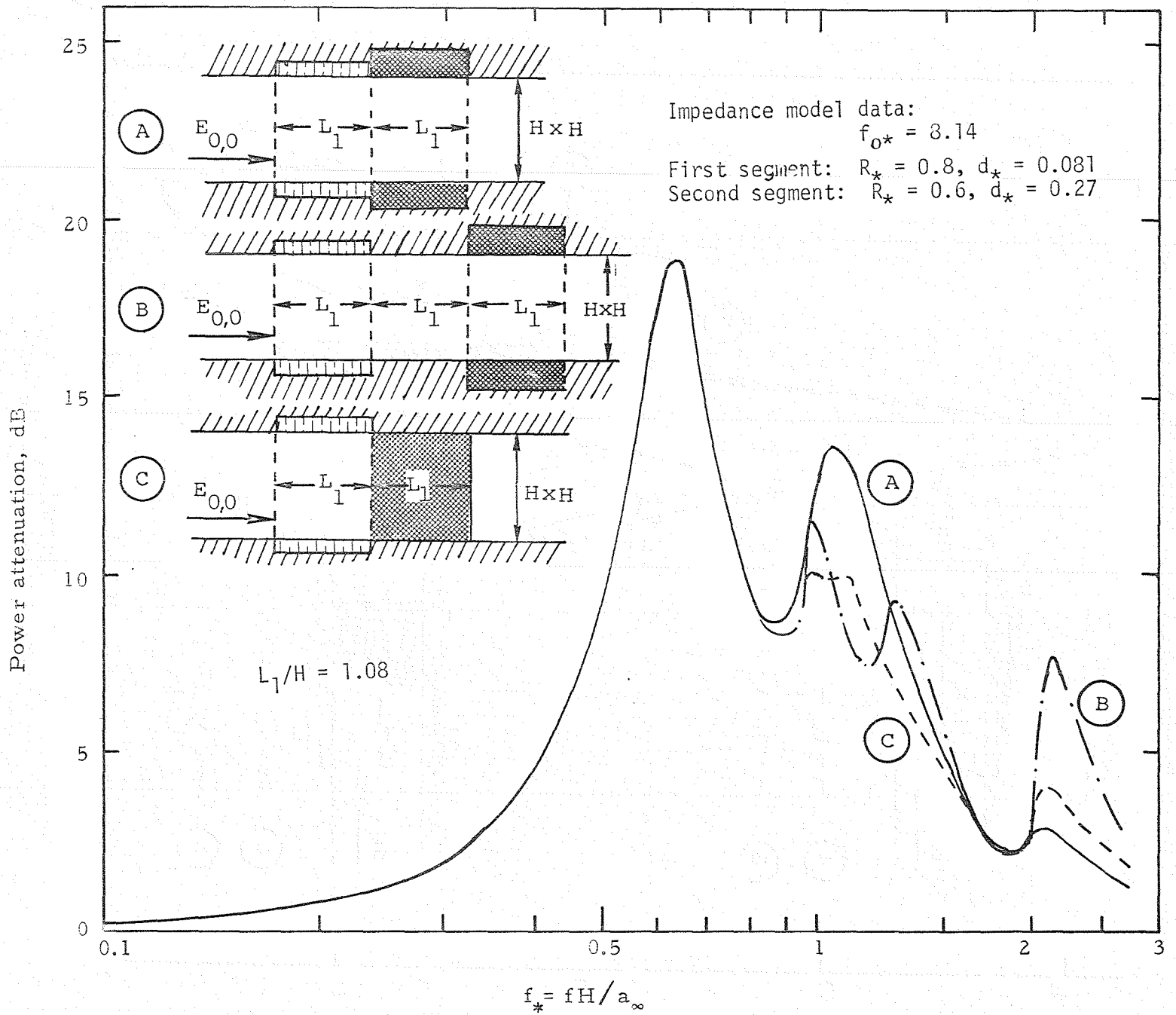

Figure 3.- Power attenuation versus frequency with (0,0) mode incident.

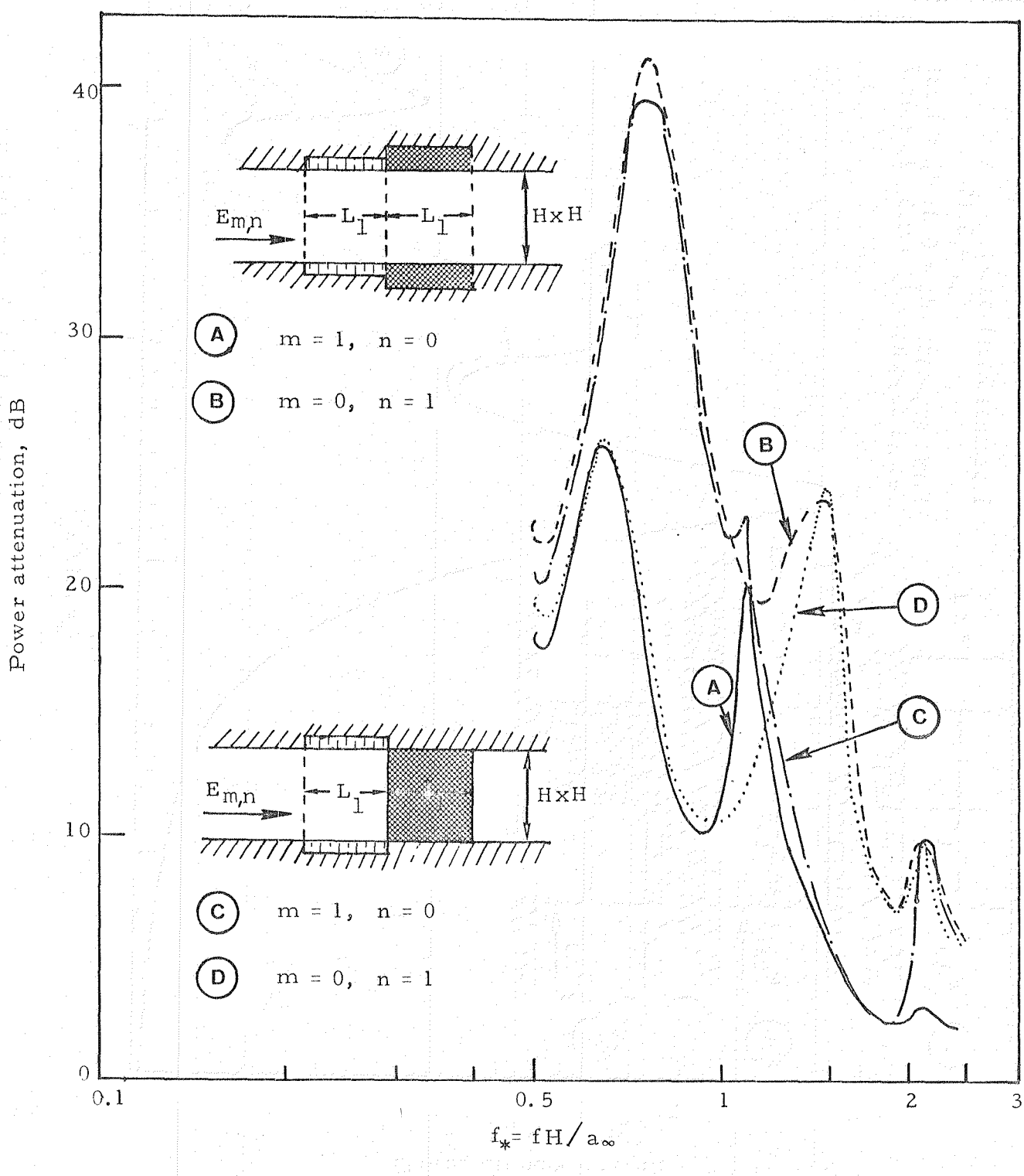

Figure 4.- Power attenuation versus frequency with (1,0) or (0,1) mode incident. (Liner data as in Figure 3).

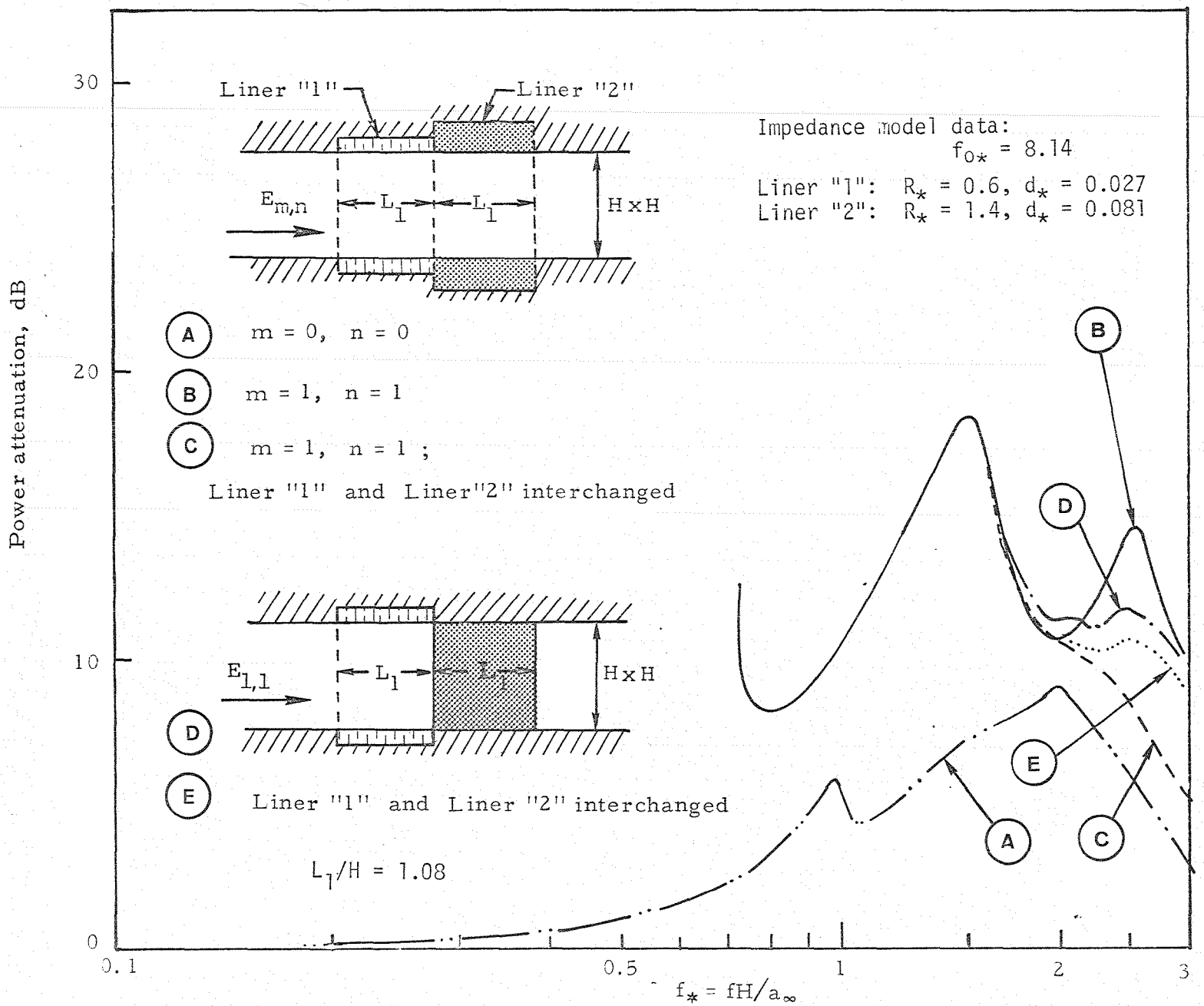

Figure 5.- Power attenuation versus frequency with (0,0) mode, (Curve A), or (1,1) mode incident.

End of Document